

Article

Standing Wave Field Distribution in Graded-Index Antireflection Coatings

Hongxiang Deng ^{1,2,*}, Xianyue Dong ¹, Huanhuan Gao ¹, Xiaodong Yuan ¹, Wanguo Zheng ¹ and Xiaotao Zu ^{2,*}

¹ Research Center of Laser Fusion, China Academy of Engineering Physics, Mianyang 621900, China; Dong_x_yue@163.com (X.D.); huanh_gao@163.com (H.G.); xdyuan@caep.cn (X.Y.); wanguo_zheng@163.com (W.Z.)

² School of Physical Electronic, University of Electronic Science and Technology of China, Chengdu 610054, China

* Correspondence: denghx@uestc.edu.cn (H.D.); xtzu@uestc.edu.cn (X.Z.); Tel.: +86-152-2890-9049 (H.D.)

Received: 8 December 2017; Accepted: 28 December 2017; Published: 4 January 2018

Abstract: Standing wave field distributions in three classic types of graded-index antireflection coatings are studied. These graded-index antireflection coatings are designed at wavelengths from 200 nm to 1200 nm, which is the working wavelength range of high energy laser system for inertial-fusion research. The standing wave field distributions in these coatings are obtained by the numerical calculation of electromagnetic wave equation. We find that standing wave field distributions in these three graded-index anti-reflection coatings are quite different. For the coating with linear index distribution, intensity of standing wave field decreases periodically from surface to substrate with narrow oscillation range and the period is proportional to the incident wavelength. For the coating with exponential index distribution, intensity of standing wave field decreases periodically from surface to substrate with large oscillation range and the period is also proportional to the incident wavelength. Finally, for the coating with polynomial index, intensity of standing wave field is quickly falling down from surface to substrate without an obvious oscillation. We find that the intensity of standing wave field in the interface between coating and substrate for linear index, exponential index and polynomial index are about 0.7, 0.9 and 0.7, respectively. Our results indicate that the distributions of standing wave field in linear index coating and polynomial index coating are better than that in exponential index coating for the application in high energy laser system. Moreover, we find that the transmittance of linear index coating and polynomial index coating are also better than exponential index coating at the designed wavelength range. Present simulation results are useful for the design and application of graded-index antireflection coating in high energy laser system.

Keywords: graded-index antireflection coating; standing wave field distribution; laser induced damage of optical coating; high energy laser system

1. Introduction

Laser systems for inertial-fusion research are required to possess the maximum possible power and energy. However, the output energy of laser system is usually limited by the damage of optical coatings and elements [1–6]. Antireflection (AR) coating is widely used in laser system, which can effectively reduce the reflection of optical elements [7–15]. There are two kinds of AR coatings. One is the multi-layers AR coating [8] and another is Graded-index AR coating [7,9,16]. It was found that, comparing to multi-layers AR coating, graded-index AR has some obvious advantages: (i) Graded-index AR coating can reduce significantly the reflection over a wide range of wavelengths [1,17,18] and angles of incidence [9], while the multi-layers AR coating is usually worked

at a specific wavelength; (ii) The laser damage threshold of Graded-index AR coating is higher than multi-layers AR coating [1]. Thus, the Graded-index AR coating attracts a lot of attention for high energy laser applications. When an incident laser beam enters into optical coating, the reflected part of this laser beam will interfere with the incident laser beam and form the standing wave. It is believed that standing wave distribution plays an important role for laser induced damage of AR coating [2] and a good design of standing wave distribution can obviously increase the damage threshold of it [19–22]. Therefore, the study of Standing wave field distribution in AR coating is important for the high energy laser systems, which can be used for inertial-fusion research and other studies of intense laser physics [22,23]. The standing wave field distribution of multi-layers AR coatings are known well. It was found that, for multi-layers AR coatings, the maximum intensity of Standing wave field is usually happened in the interfaces between layers. Because the absorption coefficients of interfaces are several orders of magnitude larger than other parts of film layer [24,25], this standing wave field distribution is bad for the resistance of laser damage. The index in graded-index AR coating is changed continuously. Thus, graded-index AR coating can avoid this problem. There are three classic graded-index AR coatings that were found to be good for reducing the reflection over a wide range of wavelengths. One is the linear distribution of index [18], the second one is exponential distribution [26,27] and the third one is polynomial distribution [26]. These graded-index AR coatings are potentially used in high laser system. So far, however, there is no study about the standing wave field distribution in these graded-index AR coatings. In this work, these graded-index AR coatings are designed at working wavelengths from 200 nm to 1200 nm, which are the working wavelengths for inertial-fusion research. The transmittance of the coatings are calculated by Fresnel coefficients matrix method. The standing wave field distributions in these three graded-index AR coatings are obtained by the numerical calculation of electromagnetic wave equation [24].

2. Theory and Model

The graded-index AR coatings for linear index distribution, exponential index distribution, and polynomial index distribution are designed at the working wavelengths from 200 nm to 1200 nm of incident laser, which is the wavelength range for inertial-fusion research. For inertial-fusion research, to possess the maximum possible energy, the incident laser is usually perpendicular to the optical elements of laser system. Therefore, we only consider the case that the incident laser is perpendicular to the coatings in this study. Fused silica is taken as the substrate of the graded-index AR coatings, which is widely used in high power laser system [6]. In our design, the maximum index of graded-index AR coatings is close to the index of fused silica ($n = 1.45$) and the minimum index is close to air ($n = 1$) [18]. The transmittance of the graded-index AR coatings are calculated by Fresnel coefficients matrix method [28,29]. To make the graded-index AR coatings working at wavelengths from 200 nm to 1200 nm, a numerical searching method is used to find the optimum matching thickness of coating. In this method, the transmittance of AR coating is the quantity to be optimized and the coating has maximum transmittance of designed wavelengths in optimum matching thickness of coating. The method is that we divide the index distribution of graded-index AR coating by many thin layers. The thickness of each thin layer is taken as d . We make the numerical search of d from 0 to d_0 , here d_0 is the maximum searching thickness of the thin layers. If the maximum transmittance of graded-index AR coating is happened as thickness of thin layers is d_1 , the optimum matching thickness of AR coating will be $N \times d_1$, where N is the number of the thin layers. Since index distribution of idea graded-index coating is continuous, to approach this ideal index distribution, the thickness of thin layers should be small and the number of the thin layers N should be large. This is a rule for thickness d and number of layers N .

Because the thickness of AR coating is less than the wavelength of incident light (e.g., the thickness of single layer AR coating is less than a quarter of wavelength), the maximum overall searching thickness of coating $N \times d_0$ can be taken as the wavelength of incident light (it is a enough maximum searching thickness and the optimize thickness $N \times d_1$ of coating is in this searching range).

It should be noted that thickness d and the number of the thin layers N are modeling parameters, but not are parameters for real fabrication. The aim of the modeling is to find the optimum matching thickness of graded-index AR coating. For real fabrication, one can redivide the obtained optimum matching thickness of AR coating. The more detailed discussion can be found in Section 3 (paragraph 3) and Section 4 (paragraph 1).

The standing wave field distribution of graded-index AR coatings are obtained by the numerical calculation of electromagnetic wave equation. The electromagnetic wave equation for a vertical incident plane wave in coating is in the form [24]

$$\frac{d^2 \vec{E}}{dz^2} + \frac{\omega^2}{c^2} \varepsilon(z) \vec{E} = 0, \quad (1)$$

where, $\varepsilon(z)$ is the relative permittivity of coating at position z . Here $z = 0$ is the surface of coating. \vec{E} , ω and c are the electric field amplitude, angular frequency of laser and velocity of light in vacuum, respectively. The boundary conditions of Equation (1) are as follows:

$$\begin{cases} \vec{E}_0^+ (1 + r) = \vec{E}(z = 0^+) \\ ik_0 \vec{E}_0^+ (1 - r) = \frac{d\vec{E}}{dz}(z = 0^+) \end{cases}, \quad (2)$$

where, $k_0 = \frac{\omega}{c}$; $r = \frac{\vec{E}_0^-}{\vec{E}_0^+}$ is reflection coefficient of coating which is obtained by Fresnel coefficients matrix method. Here, \vec{E}_0^+ , \vec{E}_0^- are the electric field amplitude of incident wave and reflect wave at the surface of coating, respectively.

3. Results

In this section, the transmittance of graded-index AR coatings with linear index distribution, exponential index distribution, and polynomial index distribution are first designed at working wavelengths from 200 nm to 1200 nm, and then the standing wave field distributions in these designed coatings are obtained by the numerical calculation of electromagnetic wave equation.

The numerical calculation of Equation (1) is conducted by fourth order Runge–Kutta method which is an effective algorithm to solve differential equations. In our calculation, for convenience, the value of electric field amplitude of incident wave at surface \vec{E}_0^+ is taken as 1 and the ratio $\frac{\vec{E}^2}{\vec{E}_0^2}$ is taken as the intensity of standing wave field.

To make the graded-index AR coatings working at wavelengths from 200 nm to 1200 nm, a numerical searching method is used to find the optimum matching thickness of coating as mentioned in Section 2. In our work, the range to optimize thickness d is taken from 0 nm to 3 nm. So, to keep the maximum searching thickness of entire coating $N \times d$ close to maximum wavelength (1200 nm) of designed wavelength range 200–1200 nm, we chose the number of layers $N = 450$ ($450 \times 3 \text{ nm} > 1200 \text{ nm}$). For searching method, the number of layers N does not need to be 450 and the specific number is not important. We also can chose $N = 700$. In this case, the range to optimize thickness d can be taken as 0–2 nm ($700 \times 2 = 1400 \text{ nm} > 1200 \text{ nm}$). The aim of the searching is to find the optimize thickness $N \times d$ of graded-index AR coating, in which the coating has maximum transmittance. For ideal graded-index coating, the index distribution is continuous. Thus, d should be much smaller than the wavelength of incident laser and it is not a thickness for real fabrication of graded-index AR coating. For real fabrication of graded-index AR coating, one can re-divide the obtained optimized thickness. Figures 1d, 2d and 3d are examples for the re-divisions of obtained optimize thickness of linear index distribution, exponential index distribution,

and polynomial index distribution, respectively. In all our re-divisions, the minimum thickness is large than 5 nm and the minimum index contrast among layers is 0.01.

3.1. Linear Distribution of Index

For the graded-index AR coating with linear index distribution [18], the index distribution is in the form

$$n(z) = n_{\min} + \frac{n_{\max} - n_{\min}}{z_{\text{tot}}} z, z \leq z_{\text{tot}} \quad (3)$$

where, n_{\min} and n_{\max} are minimum index and maximum index of graded-index AR coating, respectively. z is coordinate of coating and $z = 0$ is the surface of coating. z_{tot} is thickness of the coating.

Figure 1a shows transmittance of graded-index AR coatings with linear index distribution at different searching thickness d of divided thin layers (as mentioned in Section 2). We find that the best searching thickness is $d = 0.925$ nm as the number of divided thin layers is $N = 450$. Thus, the optimum matching thickness of entire coating is $N \times d = 0.925 \times 450$ nm.

The transmittance at best searching thickness d are shown in Figure 1b. From Figure 1b, it can be found that the transmittance are all above 99.8% at working wavelengths from 200 nm to 1200 nm. In Figure 1c, the intensity of standing wave field at wavelengths of 355 nm, 510 nm and 1064 nm are presented. From Figure 1c, it can be found that the intensity of standing wave field decreases periodically from surface to substrate and the distributions are similar for different wavelengths. The maximum intensities of these standing wave fields are near the interface between air and the coating and the minimum intensities are near the interface between the coating and the substrate. Moreover, Figure 1c shows that the period of standing wave field is proportional to the incident wavelength.

For real fabrication of this graded-index coating, one can redivide the obtained optimized matching thickness. Figure 1d is an example for re-division. In this re-division, the coating is equally divided into 45 layers. The thickness of one layer is about 9 nm and the minimum index contrast among layers is 0.01. In Figure 1d, refractive index distribution for the division with best searching thickness d is also presented. From Figure 1d, we can find that refractive index distribution for the division with best thickness d (green line) is nearly continuous and quite close to the description of Equation (3). The comparison of transmittance between division with best thickness d and the re-division with 45 layers is shown in Figure 1e. From Figure 1e, it can be seen that the transmittance curves for both divisions are quite close.

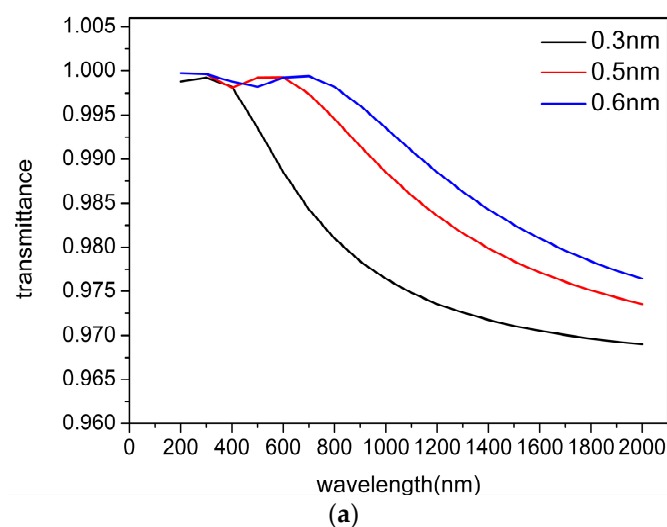


Figure 1. Cont.

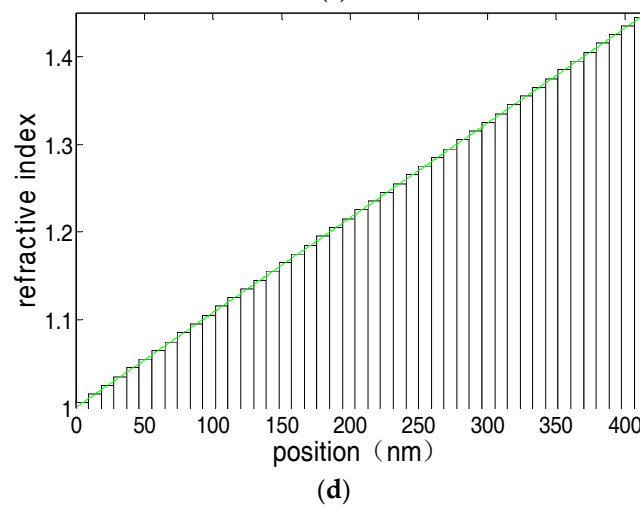
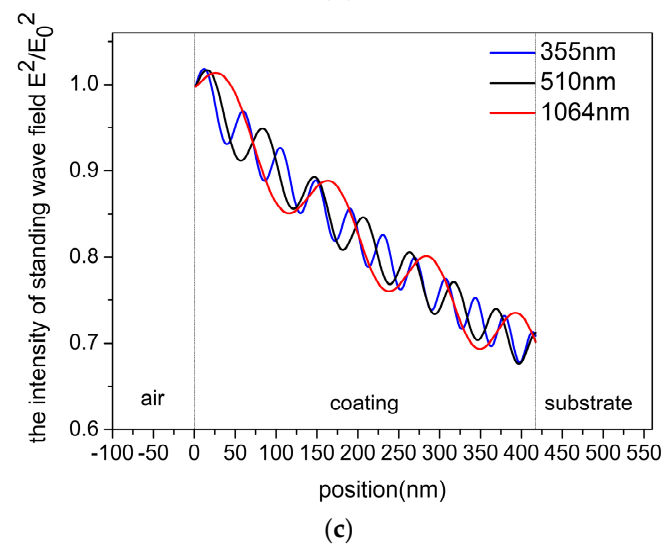
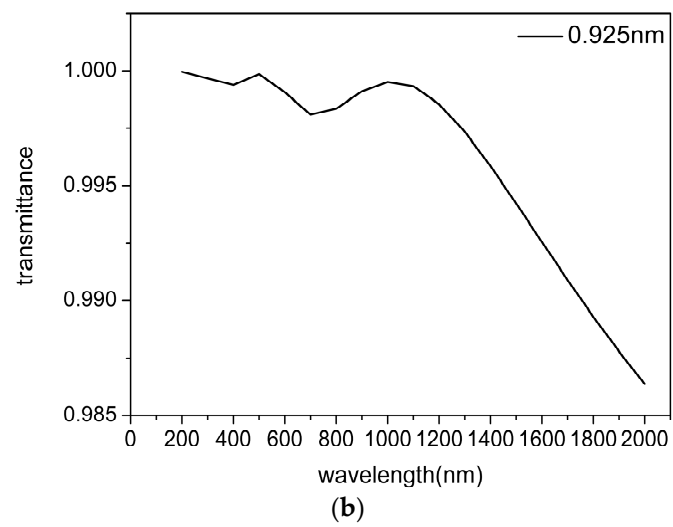


Figure 1. Cont.

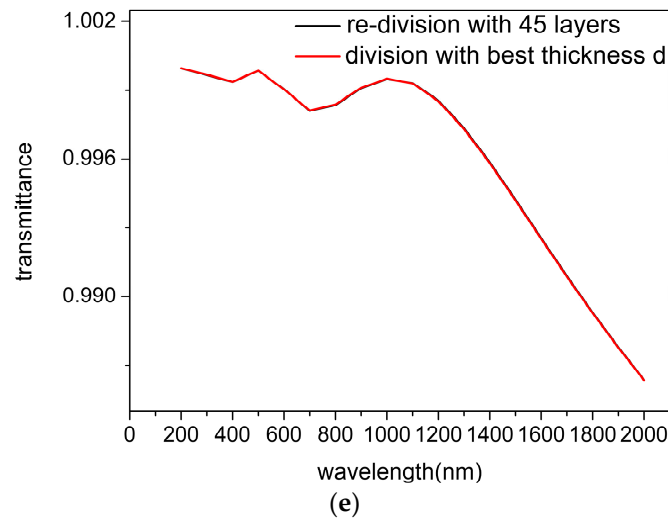


Figure 1. (a) Transmittance of graded-index AR coatings with linear index distribution at different searching thickness d of divided thin layers, the black line presents $d = 0.3$ nm, the red line presents $d = 0.5$ nm and the blue line shows $d = 0.6$ nm; (b) The transmittance at best thickness d ($d = 0.925$ nm); (c) The intensity of standing wave field for optimum matching thickness of coating at wavelengths of 355 nm, 510 nm and 1064 nm; (d) Refractive index distributions for the division with best thickness d (green line) and the re-division with 45 layers (black bars); (e) Comparison of transmittance between division with best thickness d and the re-division with 45 layers.

3.2. Exponential Distribution of Index

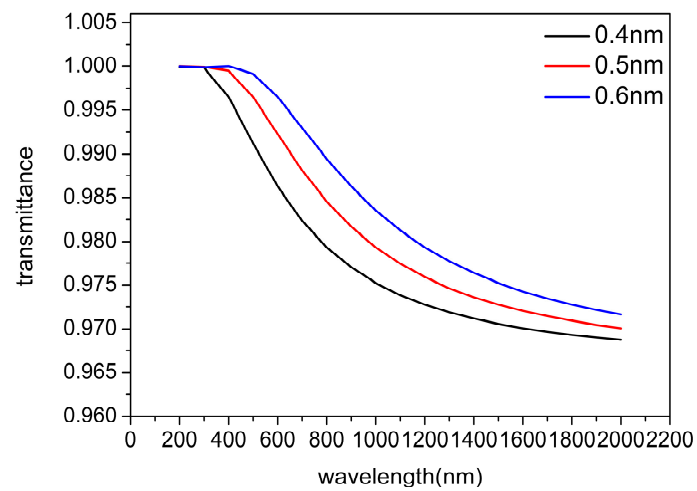
For the graded-index AR coating with exponential index distribution [18], the index distribution can be written as [26,27]

$$n(z) = n_{\max} \exp\left(\frac{1}{2} \ln\left(\frac{n_{\max}}{n_{\min}}\right) \times \left\{\sin\left[\pi\left(\frac{x}{x_{\text{tot}}}\right) + \frac{\pi}{2}\right] - \sin\frac{\pi}{2}\right\}\right), \quad (4)$$

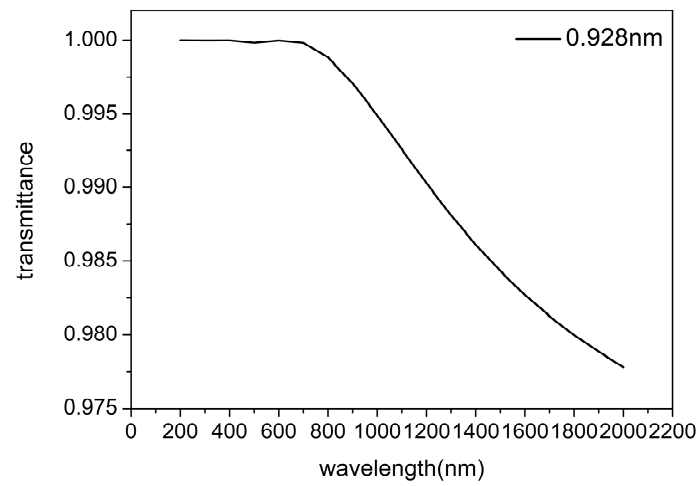
where, $x = \int_0^z n(z') dz'$, $x_{\text{tot}} = \int_0^d n(z') dz'$ are the optical distances from the substrate and total optical thickness, respectively.

Figure 2a shows transmittance of exponential index AR coatings at different thickness d of divided thin layers. We find that the best thickness of thin layer is $d = 0.928$ nm as the number of divided layers is 450. The transmittance of wavelengths from 200 nm to 2000 nm at best length d are shown in Figure 2b. From Figure 2b, it can be found that the values of the transmittance are almost equal to 1 at wavelengths from 200 nm to 700 nm. However, the transmittance is quickly down as wavelength is larger than 700 nm. The value of the transmittance at wavelength of 1200 nm is about 99%. The distributions of standing wave field at wavelengths of 355 nm, 510 nm and 1064 nm are presented in Figure 2c. From Figure 2c, we can find that the intensity of standing wave field in exponential index coating decreases periodically from surface to substrate and the period is proportional to wavelength. The standing wave field is similar to the case of linear distribution of index, but the oscillation range is much larger than linear distribution.

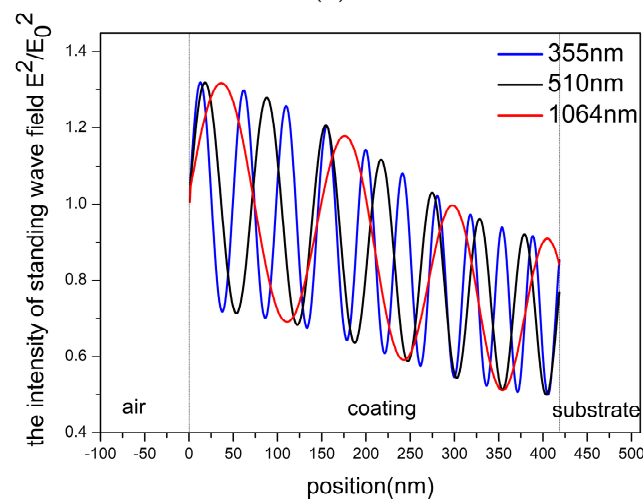
Figure 2d is an example for real fabrication. In this re-division, exponential index distribution is divided into 41 layers and the minimum thickness of one layer is about 6 nm. The index contrasts between adjacent layers is above 0.01. The comparison of transmittance between division with best thickness d and the re-division with 41 layers is shown in Figure 2e. From Figure 2e, we can find that the transmittance curves for both divisions are quite close.



(a)



(b)



(c)

Figure 2. Cont.

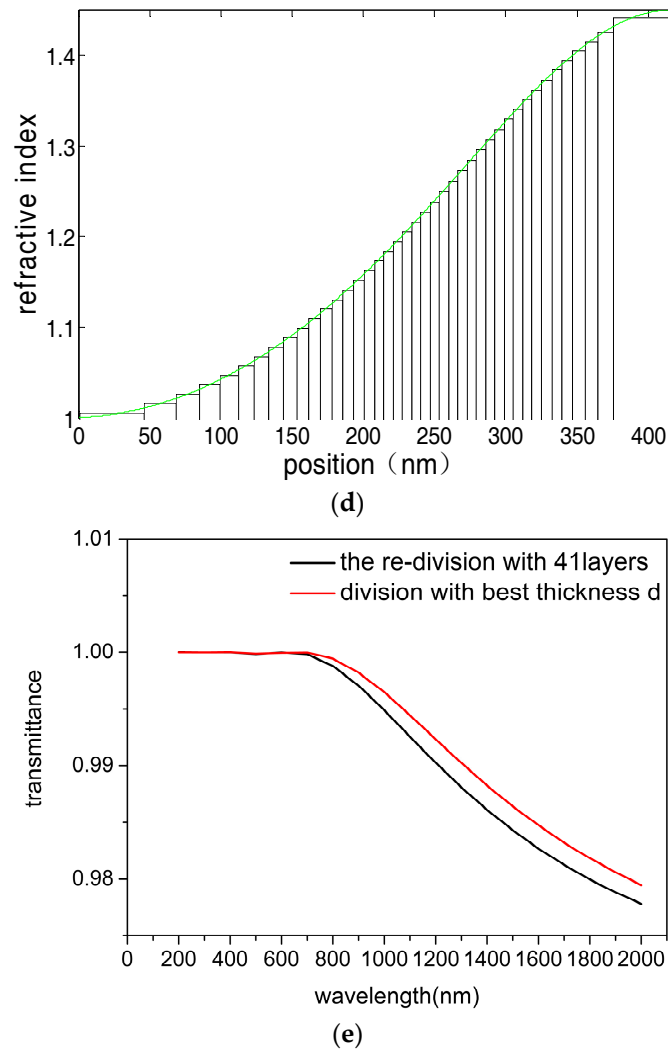


Figure 2. (a) Transmittance of exponential index antireflection (AR) coatings at different searching thickness d of divided thin layers, the black line presents $d = 0.4$ nm, the red line presents $d = 0.5$ nm and the blue line shows $d = 0.6$ nm; (b) The transmittance at best thickness d ($d = 0.928$ nm); (c) The intensity of standing wave field for optimum matching thickness of coating at wavelengths of 355 nm, 510 nm and 1064 nm; (d) Refractive index distributions for the division with best thickness d (green line) and the re-division with 41 layers (black bars); (e) Comparison of transmittance between division with best thickness d and the re-division with 41 layers.

3.3. Polynomial Distribution of Index

In the polynomial index coating, the distribution of index has the form [26],

$$n(z) = n_{\max} - (n_{\max} - n_{\min}) \left[10 \left(\frac{z}{z_{\text{tot}}} \right)^3 - 15 \left(\frac{z}{z_{\text{tot}}} \right)^4 + 6 \left(\frac{z}{z_{\text{tot}}} \right)^5 \right], \quad (5)$$

Figure 3a shows transmittance of polynomial index coating at different thickness of thin layer. It is found that the best thickness of thin layer is $d = 1.858$ nm as the number of divided layers is 450. Thus, the optimum matching thickness of entire coating is $N \times d = 1.858 \times 450$ nm. The transmittance of polynomial index coating at the best thickness are shown in Figure 3b. From Figure 3b, it can be found that the values of the transmittance are almost equal to 1 at wavelengths from 200 nm to 1200 nm. The distributions of standing wave field at wavelengths of 355 nm, 510 nm and 1064 nm are presented in Figure 3c. From Figure 3c, we can find that standing wave fields of different wavelengths are nearly

the same and the intensity of standing wave field is quickly falling down from surface to substrate. Different from linear index coating and exponential index coating, the intensity of standing wave field in polynomial index coating does not have an obvious oscillation.

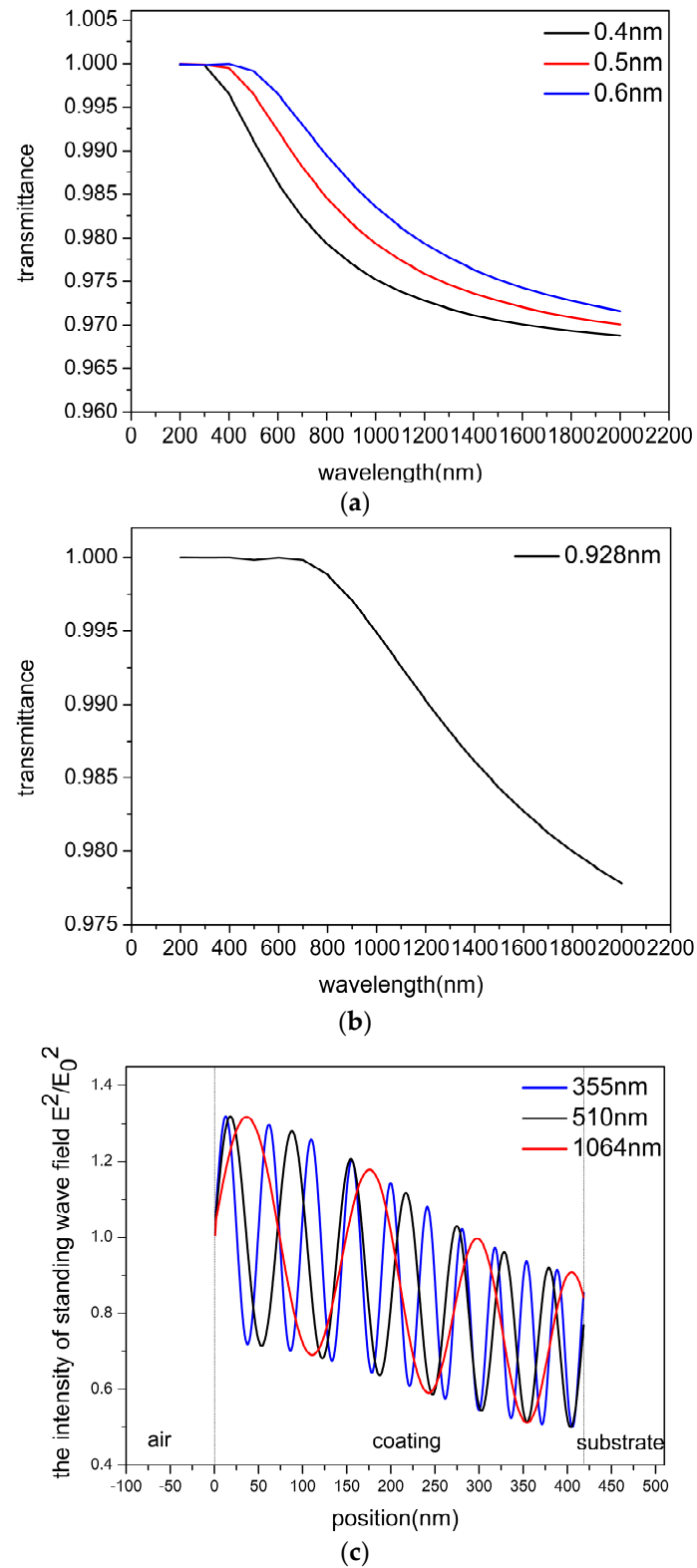


Figure 3. Cont.

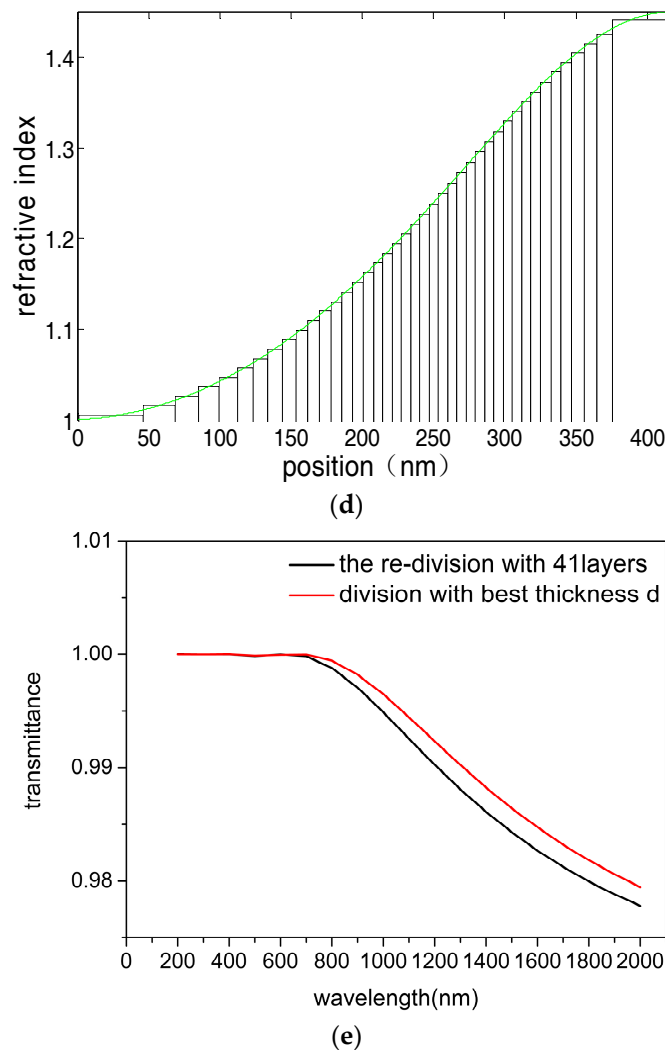


Figure 3. (a) Transmittance of polynomial index AR coatings at different searching thickness d of divided thin layers the black line presents $d = 0.5$ nm, the red line presents $d = 1$ nm and the blue line shows $d = 1.2$ nm; (b) The transmittance at best thickness d ($d = 1.858$ nm); (c) The intensity of standing wave field for optimum matching thickness of coating at wavelengths of 355 nm, 510 nm and 1064 nm; (d) Refractive index distributions for the division with best thickness d (green line) and the re-division with 42 layers (black bars); (e) Comparison of transmittance between division with best thickness d and the re-division with 42 layers.

Figure 3d is an example for real fabrication of polynomial index. In this re-division, exponential index distribution is divided into 42 layers and the minimum thickness is about 11 nm. The index contrasts between adjacent layers is above 0.01. The comparison of transmittance between division with best thickness d and the re-division with 42 layers is shown in Figure 3e. From Figure 3e, we can find that the transmittance curves for both divisions are quite close.

4. Discussion

Strictly speaking, the index distribution of idea graded-index coating is continuous. From Figures 1d, 2d and 3d, we find that refractive index distributions for the divisions at best thicknesses d (green lines) are nearly continuous and quite close to the idea index distribution which are described by Equations (3)–(5). So the results of the divisions at best thicknesses d (Figure 1b,c, Figure 2b,c and Figure 3b,c) stand for the results of idea graded-index coatings.

From Figures 1b, 2b and 3b, it can be found that transmittance are good at the designed wavelengths 200–1200 nm. It means that our simple searching method is working well.

The results from Figures 1e, 2e and 3e show that the transmittance of linear index coating, exponential index coating and polynomial index coating are not sensitive to the re-divisions. Thus, these coatings are fabricable.

As shown in Figures 1c, 2c and 3c, the intensities of standing wave field in the interface between coating and substrate for linear index, exponential index and polynomial index are about 0.7, 0.9 and 0.7, respectively. We know that the absorption coefficient of interfaces between coating and substrate are several orders of magnitude larger than other parts of coating [25], so the lower intensity of standing wave field will be helpful for the resistance of laser induced damage. It means that linear index coating and polynomial index coating have large damage thresholds than exponential index coating. Moreover, as shown in Figures 1b, 2b and 3b, the transmittance of linear index coating and polynomial index coating are also better than exponential index coating at the designed wavelengths 200–1200 nm. The transmittance of linear index coating and polynomial index coating at designed wavelengths are all above 99.8%, but for exponential index coating, the transmittance at wavelengths from 1000 nm to 1200 nm are below 99.5%. So present results indicate that linear index coating and polynomial index coating are better than exponential index coating for the application in high energy laser system.

5. Conclusions

In conclusion, transmittance and standing wave field distribution are studied for three classic kinds of graded-index AR coating which are potentially applied in high energy system.

The transmittance of these graded-index coatings are designed by a searching method which is proposed in this work. We find that the searching method is working well and transmittance of the designed coatings are good at the designed wavelengths 200–1200 nm, which are the working wavelengths for laser induced inertial-fusion research. Re-divisions for the obtained optimize thicknesses of these three kinds coatings show that the designed coatings are fabricable. Our simple searching method can be widely used to design graded-index coating.

The standing wave field distributions of these graded-index coatings are numerical calculated by the electromagnetic wave equation, which are significant for the study of intense laser induced damage of coating. We find that standing wave field distributions of these three graded-index AR coatings are quite different. For the coating with linear index distribution intensity of standing wave field decreases periodically from surface to substrate with narrow oscillation range and the period is proportional to the incident wavelength. For the coating with exponential index distribution, intensity of standing wave field decreases periodically from surface to substrate with large oscillation range and the period is also proportional to the incident wavelength. Finally, for the coating with polynomial index, intensity of standing wave field is quickly falling down from surface to substrate without an obvious oscillation. We also find that the intensity of standing wave field in the interface between coating and substrate for linear index and polynomial index are lower than exponential index. It means that linear index coating and polynomial index coating have large damage thresholds than exponential index coating. Our findings can be used to design the high damage threshold graded-index AR coating.

The present simulation results are useful for the design and application of graded-index AR coating in high energy laser system.

Acknowledgments: This work was financially supported by the Fundamental Research Funds for the Central Universities (Grant No. ZYGX2014J036); the National Natural Science Foundation of China (No. 61505023); China Postdoctoral Science Foundation funded project (No. 2015M582570 and No. 2016T90871).

Author Contributions: Hongxiang Deng, Xiaodong Yuan and Xiaotao Zu conceived and designed the study; Hongxiang Deng performed the simulation; Hongxiang Deng, Xianyue Dong, Wanguo Zheng analyzed the data; Hongxiang Deng, Xianyue Dong and Huanhuan Gao wrote the paper.

Conflicts of Interest: The authors declare no conflict of interest.

References

- Lowdermilk, W.H.; Milam, D. Graded-index antireflection surfaces for high-power laser applications. *Appl. Phys. Lett.* **1980**, *36*, 891–893. [[CrossRef](#)]
- Shunli, C.; Yuan'an, Z.; Hongbo, H.; Jianda, Z. Effect of standing-wave field distribution on femosecond laser-induced damage of HfO₂/SiO₂ mirror coating. *Chin. Opt. Lett.* **2011**, *8*, 94–97. [[CrossRef](#)]
- Li, X.; Gross, M.; Oreb, B.; Jun, S. Increased laser-damage resistance of sol–gel silica coating by structure modification. *J. Phys. Chem. C* **2012**, *116*, 18367–18371. [[CrossRef](#)]
- Yang, F.; Wenfeng, Y.; Liangcai, C.; Huanliang, C.; Zuhai, C. Optimize design of high power CO laser window coatings. *Laser J.* **2007**, *28*, 18–19.
- Mende, M.; Jensen, L.O.; Ehlers, H.; Riggers, W.; Blaschke, H.; Ristau, D. Laser-induced damage of pure and mixture material high reflectors for 355 nm and 1064 nm wavelength. In Proceedings of the International Society for Optics and Photonics, SPIE Optical Systems Design, Marseille, France, 5–8 September 2011.
- Deng, H.X.; Xiang, X.; Zheng, W.G.; Yuan, X.D.; Wu, S.Y.; Jiang, X.D.; Gao, F.; Zu, X.T.; Sun, K. Theory of absorption rate of carriers in fused silica under intense laser irradiation. *J. Appl. Phys.* **2010**, *108*, 103116. [[CrossRef](#)]
- Neuman, G.A. Anti-reflective coatings by APCVD using graded index layers. *J. Non-Cryst. Solids* **1997**, *218*, 92–99. [[CrossRef](#)]
- Bovard, B.G. Rugate filter theory: An overview. *Appl. Opt.* **1993**, *32*, 5427–5442. [[CrossRef](#)] [[PubMed](#)]
- Dobrowolski, J.A.; Poitras, D.; Penghui, M.; Himanshu, V.; Michael, A. Towards “perfect” antireflection coatings: Numerical investigation. *Appl. Opt.* **2002**, *41*, 3075–3083. [[CrossRef](#)] [[PubMed](#)]
- Masouleh, F.F.; Rozati, S.M.; Das, N. Performance improvement of plasmonic-based thin film assisted MSM-PDs. *Opt. Int. J. Light Electron Opt.* **2017**, *157*, 733–742. [[CrossRef](#)]
- Das, N.; Islam, S. Design and analysis of nano-structured gratings for conversion efficiency improvement in GaAs solar cells. *Energies* **2016**, *9*, 690. [[CrossRef](#)]
- Das, N.; Wongsodihardjo, H.; Islam, S. Modeling of multi-junction photovoltaic cell using MATLAB/Simulink to improve the conversion efficiency. *Renew. Energy* **2015**, *74*, 917–924. [[CrossRef](#)]
- Xue, S.W.; Zu, X.T.; Zhou, W.L.; Deng, H.X.; Xiang, X.; Zhang, L.; Deng, H. Effects of post-thermal annealing on the optical constants of ZnO thin film. *J. Alloys Compd.* **2008**, *448*, 21–26. [[CrossRef](#)]
- Masouleh, F.F.; Das, N.; Mashayekhi, H.R. Optimization of light transmission efficiency for nano-grating assisted MSM-PDs by varying physical parameters. *Photon. Nanostruct. Fundam. Appl.* **2014**, *12*, 45–53. [[CrossRef](#)]
- Das, N.; Ghadeer, A.A.; Islam, S. Modelling and analysis of multi-junction solar cells to improve the conversion efficiency of photovoltaic systems. In Proceedings of the IEEE Power Engineering Conference, Perth, Australia, 28 September–1 October 2014; pp. 1–5.
- Monaco, S.F. Reflectance of an Inhomogeneous Thin Film. *J. Opt. Soc. Am.* **1961**, *51*, 280–282. [[CrossRef](#)]
- Yan, Q.R.; Huang, W.; Zhang, Y.D. The gradient-index thin film design of infrared films on ZnSe Substrate for 3–12 μm . *Laser Infrared* **2008**, *38*, 177–188.
- Yan, L.H. *Study on Nanostructures and Optical Properties of Broadband Reinforced Silica Optical Thin Films*; China Academy of Engineering Physics: Mianyang, Sichuan, China, 2016.
- Apfel, J.H.; Enemark, E.A.; Milam, D. Effects of barrier layers and surface smoothness on 150-ps, 1.064- μm laser damage of AR coatings on glass. In Proceedings of the Symposium on Optical Materials for High Power Lasers, Boulder, CO, USA, 4 October 1977; Volume 18, p. 1880.
- Field, S.; Hazelwood, E.; Bourke, B.; Bourke, J.F. Multishort laser damage in transparent solids: Theory of accumulation effect. *Proc. SPIE* **1995**, *8*, e83326.
- Chen, X.Q.; Zu, X.T.; Zheng, W.G.; Jiang, X.D.; Lu, H.B.; Ren, H.; Zhang, Y.Z.; Liu, C.M. Experimental research of laser-induced damage mechanism of the sol-gel SiO₂ and ibsd SiO₂ thin films. *Acta Phys. Sin.* **2006**, *55*, 1201–1206.
- Deng, H.X.; Zu, X.T.; Xiang, X.; Sun, K. Quantum theory for cold avalanche ionization in solids. *Phys. Rev. Lett.* **2010**, *105*, 113603. [[CrossRef](#)] [[PubMed](#)]
- Gorshkov, B.G.; Epifanov, A.S.; Manenkov, A.A. Avalanche ionization produced in solids by large radiation quanta and relative role of multiphoton ionization in laser-induced breakdown. *J. Exp. Theor. Phys.* **1979**, *49*, 309.

24. Deng, H.X.; Zu, X.T.; Zheng, W.G. Gradient optical film taking the place of classical high-reflectivity film. *High Power Laser Part. Beams* **2007**, *19*, 58–62.
25. Zhao, Q.; Fan, Z.X. Effect of optical film interface absorption on temperature field. *Acta Opt. Sin.* **1996**, *16*, 777–782.
26. Poitras, D.; Dobrowolski, J.A. Toward perfect antireflection coatings—2. Theory. *Appl. Opt.* **2002**, *41*, 3075–3083. [[CrossRef](#)]
27. Xiaolan, L. Design and Preparation of TiO₂-Based Anti-Reflection Films. Master's Thesis, Hunan University, Changsha, China, 25 May 2011.
28. Monaco, S.F. Homogeneous—In-homogeneous thin-film combinations. *J. Opt. Soc. Am.* **1961**, *51*, 855–858. [[CrossRef](#)]
29. Lin, Y.C. *Principles of Optical Film*; National Defense Industry Press: Beijing, China, 1990.



© 2018 by the authors. Licensee MDPI, Basel, Switzerland. This article is an open access article distributed under the terms and conditions of the Creative Commons Attribution (CC BY) license (<http://creativecommons.org/licenses/by/4.0/>).